ARMin

A robot for patient-cooperative arm therapy

Originally published in:
Medical & Biological Engineering & Computing 45(9), https://doi.org/10.1007/s11517-007-0226-6

Med Bio Eng Comput (2007) 45:887-900
DOI 10.1007/s11517-007-0226-6

ORIGINAL ARTICLE

ARMin: a robot for patient-cooperative arm therapy

Tobias Nef · Matjaz Mihelj · Robert Riener

Received: 22 December 2006 / Accepted: 1 July 2007 / Published online: 3 August 2007

Abstract Task-oriented, repetitive and intensive arm training can enhance arm rehabilitation in patients with paralyzed upper extremities due to lesions of the central nervous system. There is evidence that the training duration is a key factor for the therapy progress. Robot-supported therapy can improve the rehabilitation allowing more intensive training. This paper presents the kinematics, the control and the therapy modes of the arm therapy robot ARMin. It is a haptic display with semi-exoskeleton kinematics with four active and two passive degrees of freedom. Equipped with position, force and torque sensors the device can deliver patient-cooperative arm therapy taking into account the activity of the patient and supporting him/her only as much as needed. The haptic display is combined with an audiovisual display that is used to present the movement and the movement task to the patient. It is assumed that the patient-cooperative therapy approach combined with a multimodal display can increase the patient's motivation and activity and, therefore, the therapeutic progress.

Keywords Robotics · Haptic device · Exoskeleton · Rehabilitation · Arm therapy

T. Nef (✉) · M. Mihelj · R. Riener
Sensory-Motor Systems (SMS) Laboratory,
ETH Zürich, TAN E, Tannenstrasse 1,
8092 Zurich, Switzerland
e-mail: nef@mavt.ethz.ch
URL: www.armin.ethz.ch

T. Nef · M. Mihelj · R. Riener
Spinal Cord Injury Center, University Hospital Balgrist,
University Zurich, Zurich, Switzerland

1 Introduction

1.1 Clinical background and rationale for arm therapy

Patients with paralysed upper extremities due to lesions of the central nervous system, e.g. after stroke, traumatic brain or spinal cord injury, often receive arm therapy. The goal of this therapy is to recover motor function, improve movement co-ordination, learn new motion strategies, so called trick movements, and to prevent secondary complications, such as muscle atrophy, osteoporosis, joint degeneration and spasticity.

Several studies prove that arm therapy has positive effects on the rehabilitation progress of stroke patients (see [25] for review). Several groups observed that longer daily training sessions and longer overall training periods have a positive effect on the motor function of the arm [18, 19, 33]. In a meta-analysis comprising nine controlled studies with 1,051 stroke patients, Kwakkel et al. [17] showed that increased training intensity yields moderate positive effects on neuromuscular function and activities of daily living (ADL). The study did not distinguish between upper and lower extremities. The conclusion that the rehabilitation progress depends on training intensity and training duration supports the application of robot-aided arm therapy.

There is further evidence that machine-delivered therapies can enhance the treatment [1, 5, 20, 21, 32]. Considering upper limb therapies, a robot can provide assistance with varying degrees of compensatory movements for the affected limb. There is evidence that the recovery is more effective when the patient actively participates in the training [13]. It is hypothesized that for a successful rehabilitation, it is crucial to motivate the patient to actively participate during the training exercises.

New actor, sensor, and control strategies can make robots "intelligent" providing measurement data to assess the rehabilitation progress, and to gain insight into the underlying pathology and allowing the patient to actively participate in the training.

1.2 Rationale for robot-aided arm therapy

One-to-one manually assisted training has several limitations. The training is labour-intensive, time consuming, and, therefore, expensive. The disadvantageous consequence is that the training sessions are often shorter than required for an optimal therapeutic outcome. Finally, manually assisted movement training lacks repeatability and objective measures of patient performance and progress.

In contrast, with automated, i.e. robot-assisted, arm therapy, the duration and number of training sessions can be increased, while reducing the number of therapists required per patient. A long-term automated therapy appears to be the only way to make intensive arm training affordable for clinical use. As the actual version of the ARMin-robot is still in the prototype phase, safe operation requires that one therapist supervises the training (c.f. 2.10). In the future, it will be possible that the patient can be treated by the device with less supervision. Therefore, the therapist will be able to manage several robotic devices or he will be able to do other work besides. Thus, personnel cost can be reduced. Furthermore, the robot provides quantitative measures, thus, supporting the observation and evaluation of the rehabilitation progress.

Several groups have proposed robots to assist physiotherapy and rehabilitation of the upper limbs (see [26, 27] for review). The devices provide a varying degree of assistance to the patient's movements, ranging from no assistance if the patient has sufficient voluntary control, to full assistance, where the patient can behave passively. New control strategies have been introduced that allow the machine to comply with forces exerted by the patient enabling new possibilities for rehabilitation while guaranteeing safety for the patient [4, 27, 28].

1.3 Requirements for a rehabilitation robot

In the design and application of rehabilitation robots, medical aspects must be taken into account to ensure a successful training. It is crucial that the robot is adaptable to the human limb in terms of segment lengths, range of motion and the number of degrees-of-freedom (DOF). A high number of DOF allows a wide variety of movements, with many anatomical joint axes involved. However, this can make the device complex, inconvenient and expensive. It remains an open issue to assess how many DOF are optimal for upper limb rehabilitation. The question is whether therapeutic outcome can be maximized, if the robot acts on the entire extremity rather than on single joints only. To answer this question would require a clinical study of an enormous sample size performed with various devices. However, there is evidence that a therapy focussing on activities of daily living (ADL) not only increases the patient's motivation but also yields an improved therapeutic outcome, compared to therapies focussing on single joint movements [2, 22, 25, 34]. To allow ADL training, a robot must be able to move the patient's arm in all relevant degrees of freedom and to position the human hand at any given point in space. This can be achieved by an end-effector-based robot or by an exoskeleton-type device.

End-effector-based robots are connected with the patient's hand or forearm at one point. From a mechanical point of view, these robots are easier to realize and thus, many research groups work with end-effector-based devices [7, 9, 16]. In contrast, the structure of exoskeleton robots resembles the human arm anatomy [29]. Consequently, the arm is attached to the exoskeleton at several points. Adaptability to different body sizes is easier in an end-effector-based system, i.e. where the robot moves the arm by inducing forces only on the patient's hand. In contrast, exoskeletal systems are more difficult to adjust, because each robot link must be adjusted to the corresponding patient arm segment. However, the advantage of an exoskeleton system as compared to the end-effector-based approach is that the arm posture is statically fully determined. Torques applied to each joint can be controlled separately and hyperextensions can be avoided by mechanical stops. The possibility to control torques in each joint separately is essential, e.g. when the subject's elbow flexors are spastic. This involuntary muscle activation results in an increased resistance against movements. To overcome the resistance, elbow torque up to 20 Nm is necessary (Table 1). This must not induce any reaction torques or forces in the shoulder joint, which can be guaranteed by an exoskeleton robot but not by an end-effector-based one. This is important because the shoulder girdle is a rather instable joint and the head of the humerus bone is held in its position by muscles and tendons and not by ligaments and bones. If one applies high shear forces to the shoulder joint, humerus head dislocation can occur.

That's the reason why therapists use both hands when they mobilize a spastic elbow joint. With the goal to avoid exercise forces to the shoulder, one hand holds the lower arm while the other hand holds the upper arm—comparable to exoskeleton robots with a cuff fixed to the lower arm and a cuff fixed to the upper arm.

Table 1 Requirements for the range of motion (ROM), velocity and the maximal torques

Axis	ROM	Velocity (°/s)	Acceleration (°/s^2)	Torque (Nm)
Axis 1 (Vertical shoulder rotation)	100° to −135°	71	103	20
Axis 2 (Horizontal shoulder rotation)	135° to −45°	60	129	20
Axis 3 (Internal/external shoulder rotation)	−50° to 95°	150	245	10
Axis 4 (Elbow flexion/extension)	0° to 135°	91	116	20

1.4 Patient cooperative arm therapy and specific research aims

Since the therapy progress depends on training intensity and training duration, the motivation of the patient turns out to be a key factor for an efficient rehabilitation [14]. The patient needs to get motivated to contribute actively to the movement, which may enhance recovery. In addition, to make longer training duration and more training sessions possible, it is crucial that the patient enjoys the therapy, stays concentrated, and does not get bored.

The so called "cooperative arm therapy" discussed in this paper takes into account the following key aspects that motivate the patient: (1) the device stimulates the three most important sensory modalities of the patient, i.e. the haptic, visual and auditory senses and (2) the robot and the patient cooperate and interact, i.e. the robot assists the patient just as much as needed to perform a particular movement task.

While many clinical studies (see [26] for review) have been conducted with end-effector-based robots with limited possibilities to control position and orientation of the human arm in the three-dimensional space, not much clinical evidence has been reported from work with actuated arm-exoskeleton robots. The key aspects of this project are that the ARMin device allows precise joint actuation and 3D movement of the arm, that the device allows to work in "patient cooperative" control modes and that the device includes a comprehensive audiovisual user interface.

2 Methods

2.1 Specifications

Training of ADL includes tasks like eating, drinking, combing hair, etc. For most of these ADL tasks, the hand has to reach a point in space, grasp an object, and then control position and orientation of the object until the task is completed. Therefore, the robot must be able to support movements of the shoulder, the elbow, and the wrist. Approximating the shoulder by a three-DOF ball-and-socket joint, and allowing elbow flexion/extension, pro/supination of the lower arm and wrist flexion/extension, results in a device with at least six active DOF. To simplify the task, our first prototype was built only with four active DOF supporting the movements of the shoulder joint and elbow flexion/extension.

The range of motion (ROM) must match as close as possible the ROM of the human arm [35]. In order to obtain a satisfactory control performance of patient-cooperative control strategies, which are based on impedance and admittance architectures, the robot must have low inertia, low friction and negligible backlash. Furthermore, the motor/gear unit needs to be back drivable. Back-driveability is required for good performance of the impedance control [10–12] and it is advantageous for the safety of exoskeleton robots (cf. 2.10).

The required velocities and accelerations have been determined by measuring the movements of a healthy subject during two ADL tasks (eating soup and manipulating a coffee cup). These values served as inputs for a simple dynamic model applied to estimate the required joint torques. In order to ensure that the robot will be strong enough to overcome resistance from the human against movements due to spasms and other complications that are difficult to model, rather high values have been selected (Table 1). The required end-point payload is 1 kg and end-point position repeatability is 10 mm. These values allow manipulation of objects like a coffee cup.

Furthermore, it is required that the robot is easy to handle and that safety is always guaranteed for both patient and therapist.

2.2 Kinematics

A semi-exoskeleton solution has been selected for the mechanical structure of the robot called ARMin (Fig. 1). The robot is fixed via an aluminium frame at the wall with the patient sitting in a wheelchair, placed beneath. The patient's torso is fixed to the wheelchair with straps and bands (Fig. 8). ARMin comprises four active and two passive DOF in order to enable elbow flexion/extension and spatial shoulder movements [24]. The distal part is characterized by an exoskeleton structure, with the patient's lower and upper arm placed inside orthotic shells.

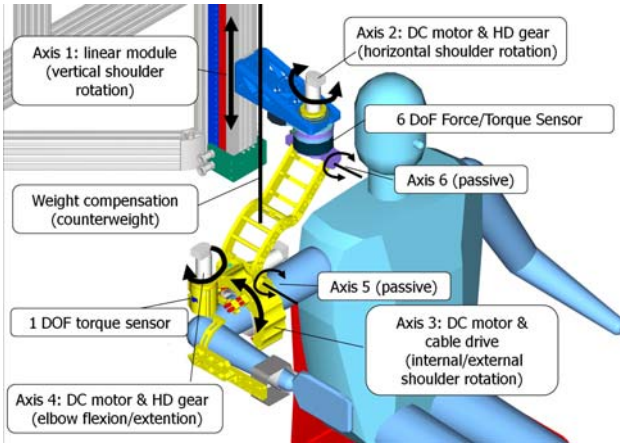

Fig. 1 Mechanical structure of ARMin [24]

The exoskeletal part drives the internal/external rotation of the upper arm and the elbow joint, whereas horizontal and vertical shoulder rotation is actuated by an end-effector-based part connecting the upper arm with the wall-mounted axes 1 and 2.

The robot becomes statically determined only in combination with the human arm. To prevent the robot from falling down and to avoid unfavourable shear forces and torques onto the human shoulder, the weight of the robot is compensated by a passive counterweight. This is achieved by a counterweight of 2.5 kg that is connected to the robot via a cable guided by two pulleys.

This end-effector-type kinematics for the shoulder joint has been selected as exoskeleton mechanics would make it difficult to get the robot axes in alignment with the anatomical axes of the human, and misalignments would mechanically overstress and potentially harm the shoulder.

2.3 Mechanics and actuation

The vertically oriented linear motion module (axis 1) drives vertical shoulder rotation (flexion/extension and abduction/adduction) movements. Horizontal shoulder rotation (horizontal flexion/extension and horizontal abduction/adduction) is realized by a backlash-free and back-drivable harmonic drive module attached to the slide of the linear motion module (Table 2).

The interconnection module connects the horizontal shoulder rotation drive with the upper arm rotary module via two hinge bearings. Elbow flexion/extension is realized by a harmonic drive rotary module.

Internal/external shoulder rotation is achieved by a special custom-made upper arm rotary module that is connected to the upper arm via an orthotic shell. For easy access to the patient's arm, the module is made out of two half-cylinders. An inner half-cylinder (Fig. 2) is guided by 32 ball bearings fixed to the exterior wall. It is actuated by three steel cables fixed to the two ends of the cylinder and rolled around the extension of the motor shaft. This guidance allows transfer of static loads in several DOF while remaining backlash-free and enabling low friction circular motion. Custom-made cuffs (Fig. 3) ensure a comfortable fixation of the patient to the arm rotary module.

2.4 Adaptation to different body sizes

To apply the robot to patients of different sizes, the lengths of exoskeleton segments need to be adjustable. Table 3 and Fig. 4 show the ranges of all possible adaptations.

In order to fix the shoulder position of the patient under the fulcrum at axis 2 (horizontal shoulder rotation), an individually adjustable belt system was constructed (Fig. 9). An optional hand support (Fig. 4) can be added to allow comfortable hand posture.

2.5 Sensors and control hardware

The four exoskeleton actuators are equipped with optical incremental sensors and redundant potentiometer-based sensors for position measurements. A six-DOF force-torque sensor beneath the horizontal arm rotation module measures forces and torques of the shoulder joint (axis 1–3). The elbow torque is measured by a separate torque sensor (Fig. 1).

The controller runs on a Matlab/Simulink XPC target (The Mathworks, Inc., USA) computer with 1 ms loop time. Four analogue channels provide inputs for the current amplifiers (Maxon 4-Q-DC Servoamplifier ADS 50/5; Maxon Motor AG, Switzerland). The four-encoder signals, the analogue signals from the redundant potentiometer-

Table 2 Actuation of the four axes

Axis	Gear	Motor type
Axis 1: Vertical shoulder rotation	Ball screw, 10 mm/rot	Maxon RE40, brushed DC
Axis 2: Horizontal shoulder rotation	Harmonic drive 1:100	Maxon RE35, brushed DC
Axis 3: Internal/external shoulder rotation	Cable drive 1:24.5	Maxon RE40, brushed DC
Axis 4: Elbow flexion/extension	Harmonic drive 1:100	Maxon RE35, brushed DC

Fig. 2 Upper arm rotary module for internal/external shoulder rotation (opened to allow view inside)

Fig. 3 Cuff that connects the rotary module with the human upper arm

Table 3 Ranges of the adaptations to different body sizes

Label	Description	Range (cm)
a	Shoulder height of the sitting patient	90–110
b	Upper arm length	27–42
c/d	Lower arm length	20–32
e	Wrist circumference	16–24
F	Upper arm circumference	20–40
G	Optional hand support	–

based position sensors are interfaced to the Sensoray 626 I/O (Sensoray Company Inc., USA) interface card.

The graphical user interface runs on a computer with Windows operating system (Microsoft Corporation, USA) and is connected with the real time target by a local area network using TCP/IP protocol.

Two graphical displays are used: (1) the therapist robot interface (TRI)—a standard LCD monitor display, and (2) the patient robot interface (PRI)—a double-projector system with polarized images to generate graphical 3D

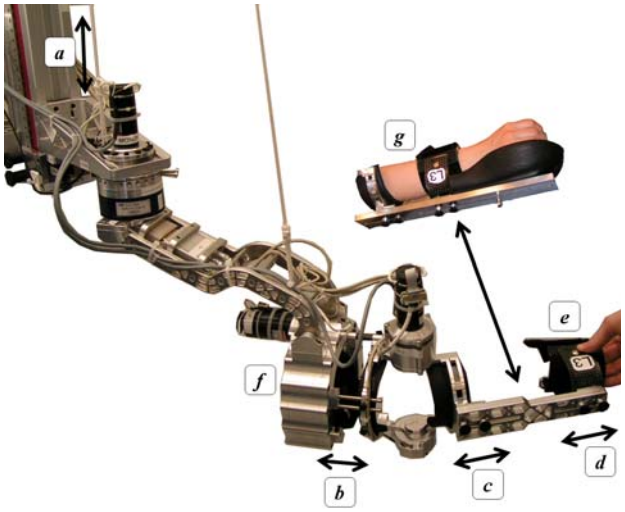

Fig. 4 Six possibilities to adapt the robot to different body sizes

scenarios for the patient. The TRI contains a dialog-based graphical user interface, which allows the therapist to enter the patient's data, choose the therapy mode, display the actual patient performance and save the therapy log file. These data are not shown to the patient, who, instead, looks onto the screen of the PRI, where the tasks are displayed by animated 3D scenarios (Fig. 6).

2.6 Dynamic model and basic control issues

A dynamic model of the robot and the human arm has been developed to simulate and evaluate different control schemes. An inverse dynamic and a direct dynamic model have been derived using Lagrange methodology. The direct dynamic model is given by

$$\ddot{\underline{q}} = M^{-1}(\underline{q})(\underline{\tau} - C(\underline{q}, \dot{\underline{q}})\dot{\underline{q}} - G(\underline{q})) \quad (1)$$

where M is the inertia matrix, $C(\underline{q}, \dot{\underline{q}})\dot{\underline{q}}$ is the vector of Coriolis and centrifugal torques, $G(\underline{q})$ is the vector of gravity torques and $\underline{q}$ is the vector of joint positions. The elements of the robot have been modelled in 3D and the matrices of inertia and the centres of gravity have been calculated using the CAD numerical finite element calculation (AutoCAD, Autodesk, USA). The upper arm and the lower segments of the human arm have been modelled as conical frustums with homogeneous mass, equal to that of water [8].

The inverse dynamic model can be expressed by

$$\underline{\tau} = M(\underline{q})\ddot{\underline{q}} + C(\underline{q}, \dot{\underline{q}})\dot{\underline{q}} + G(\underline{q}) \quad (2)$$

where $\underline{\tau}$ is the vector of joint torques. In general, the following torque contributions appear [31]

$$\tau_i = \tau_{mi} - \tau_{fi} - \tau_{hi} \quad (i = 1, \ldots, 4) \tag{3}$$

where τ_i is the driving torque of joint i, τ_{mi} is the torque of joint i delivered by the motor, τ_{fi} is the torque of joint i due to joint friction and τ_{hi} is the torque of joint i caused by the human. The velocity dependent part of friction has been identified and compensated.

A PD controller with a computed torque feed forward portion has been implemented for position control and evaluated by simulation (Fig. 5). Three different strategies have been compared regarding their control error and the computational effort with regard to the number of operations needed per time step. Sample time was fixed to 1 ms. In the first strategy, the PD values where selected by simulation and remained constant while the feed forward part was calculated by the inverse dynamic approach (Eq. 2) (computed torque control). In the second strategy, the feed forward part was simplified to the gravity part leading to

$$\underline{\tau}_{ff} = G(\underline{q}) \tag{4}$$

And in the third strategy the feed forward part has been set equal to $\underline{\tau}_{ff} = 0$, which reduces the strategy to a simple PD controller. Sinusoidal trajectories have been used for these experiments, while in the real application the trajectory generation described in Chap. 2.7 has been used. The model served also to investigate stability of the robot interacting with the human. For this purpose, a human that produces perturbations of different frequencies and amplitudes has been simulated.

2.7 Trajectory generation for the mobilisation therapy

Mobilisation therapy is based on repetitive movements of the human arm on a patient-specific trajectory while the patient remains passive. This can prevent joint degeneration, preserve the patient's mobility and joint flexibility, and reduce spasticity. The mobilisation therapy is executed in two steps. First, the therapist moves the patient's arm together with the robot on a desired trajectory. The exact shape of the movement (ranges, speed) can be solely defined by the therapist taking into consideration the individual impairment of the patient. During the recording phase, the robot's gravity and friction are compensated so that the therapist only feels the forces and torques necessary for moving the human arm. Once the trajectory is recorded, the relevant points of the trajectory are determined in order to enable calculation of a smooth and "human-like" movement path. This is required as the trajectory performed by the therapist is often shaky. Simple low-pass filtering is not appropriate, as it would cut the movement at the extremes. In the second step, the robot repeats the trajectory with an adjustable velocity.

Jung-Hoon et al. [15] developed a simple method to extract a small number of way-points for the trajectory of a mobile robot. This method has been adapted in the way that turning points of the recorded position data are detected and used as via points. Once these points are detected, a smooth trajectory connecting them is generated by a minimum jerk approach [6]. This approach is quite common to describe the kinematics of smooth human arm reaching movements. The resulting trajectory serves as input for the position controller (c.f. 2.6).

2.8 Audiovisual display

An appropriate audiovisual display is imperative for the *game supported therapy* (cf. 2.9) where movement tasks need to be displayed to the patient. The *mobilisation therapy* (cf. 2.6) could also be performed without any audiovisual feedback. However, showing a virtual arm can help the patient to realize his or her arm posture.

As the robot is able to perform ADL-related movements in space, a stereographic display is used to present virtual objects in three dimensions. The screen is rather large (2 m × 2.7 m) so that even patients with mild visual impairments can recognize the scenarios and tasks, and

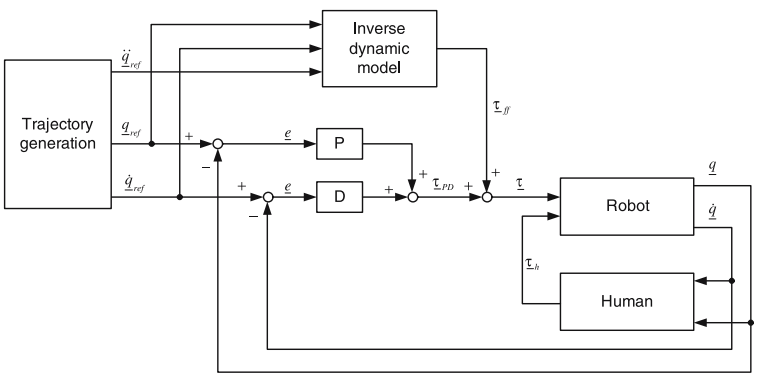

Fig. 5 Computed torque position control loop for the mobilisation therapy

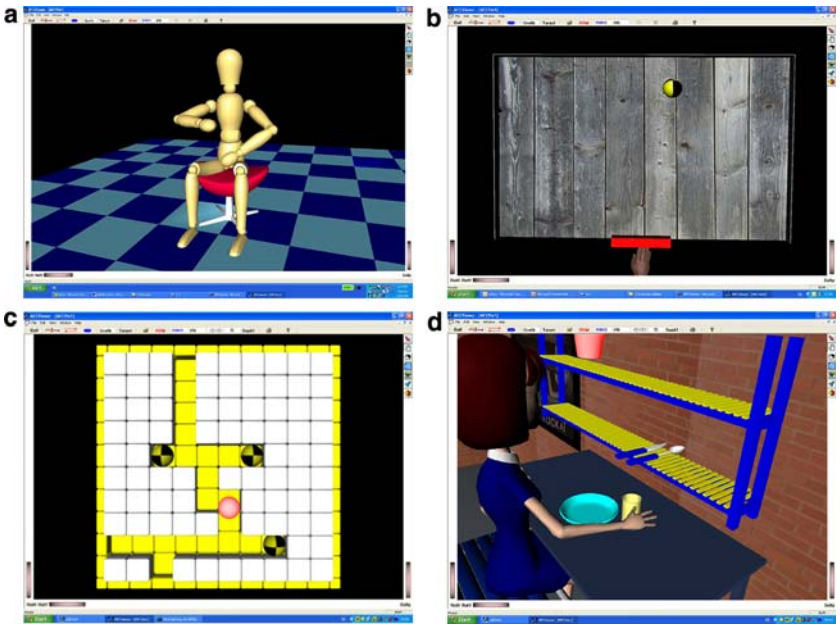

Fig. 6 Scenarios for the arm therapy. *Upper left* Movement therapy. *Upper right* Game supported therapy (ball game). *Lower left* Game supported therapy (labyrinth game). *Lower right* ADL training scenario

generate a feeling of presence. Additional sound can help to increase the feeling of presence during the *game supported therapy*.

Two projectors with polarizing filters are used to project stereographic images via back projection onto the screen. Patients wear lightweight passive polarizing glasses to see 3D images. The Open Inventor clone Coin 3D (http://www.coin3D.org) has been used as a scene graph. In combination with the quad buffer of the NVIDIA Quadro Fx 4000 graphic card (NVIDIA Corporation, USA) stereoscopic images are generated without any additional programming effort.

The virtual environment (VE) consists of a graphical, an acoustic, and a physical model of the scene. The physical model is required to determine force feedback signals in order to allow the patient to physically interact with the VE. It is implemented on the real time computer (XPC Target) and updated with a sampling rate of 1 kHz. The graphical model is implemented with Coin 3D and runs on a Windows computer with a sampling rate of approximately 100 Hz.

Several different scenarios have been implemented. During the mobilisation therapy, an avatar figure showing the actual posture of the patient's arm is presented (Fig. 6 upper left). A ball game scenario (Fig. 6 upper right) includes a ball rolling down an inclined table and a hand connected to the handle. The ball is reflected by the walls and the patient's task is to catch the ball with the handle. The colour of the handle changes depending on the performance of the patient (Fig. 11). The sounds of the rolling ball and the collisions with the wall and the handle are displayed to increase the level of realism. A labyrinth game scenario has been implemented (Fig. 6, lower left) with a red ball indicating the cursor that moves according to the patient's spatial hand movement. Force feedback is provided whenever the cursor touches the wall of the labyrinth. To motivate the patient, objects can be collected on the way from the bottom to the top of the labyrinth.

In the ADL training mode, the patient is asked to grasp an object by approaching it with the virtual hand and to put it onto the table (Fig. 6, lower right). The control strategy for these kinds of tasks is based on the minimal intervention principle, which allows an efficient exploitation of task space redundancies and results in user-driven movement trajectories [23]. The basic idea of this approach is that deviations from the trajectory are corrected only when they interfere with the task performance. In other words: if the patient is doing "better" than the robot, then the robot lets the patient do so.

2.9 Control scheme for the ball game

A simple ball game has been implemented to demonstrate and validate the concept of game-supported therapy. The task is to catch a virtual ball rolling down an inclined virtual table (Fig. 6, upper right). The ball movement in y direction (vertical direction on the screen) is governed by Newton's law:

$$v_{y_{\text{ball}}} = v_0 - g\sin(\alpha) \tag{5}$$

where v_0 is the initial velocity of the ball, g is the gravity acceleration and α is the inclination of the virtual table. The initial velocity v_0 and inclination α can be adjusted for each

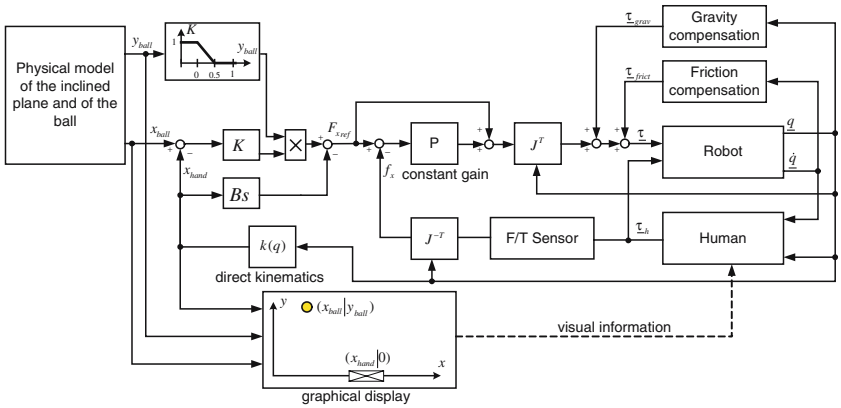

Fig. 7 Control strategy and signal flow of the ball game

patient in order to increase or decrease the difficulty of the game.

The control strategy (Fig. 7) is based on an impedance controller, where the assisting force $F_{x\text{ref}}$ is determined, based on the relative distance between the ball and the human hand position. The force in horizontal direction $F_{x\text{ref}}$, that the robot exerts onto the patient's arm to push him towards the ball position is:

$$F_{x\text{ref}} = \begin{cases} 0 & \text{if } y_{\text{ball}} > 0.5 \\ K(x_{\text{ball}} - x_{\text{hand}}) \cdot (1 - y_{\text{ball}}) - B\frac{dx_{\text{hand}}}{dt} & \text{if } y_{\text{ball}} \leq 0.5 \end{cases} \quad (6)$$

K is a constant value that can be adjusted by the therapist and B is a damping factor. Typical values are K = 10 N/m and B = 0.01 Ns/m.

During the first part of the rolling-down sequence ($y_{\text{ball}} > 0.5$), the force $F_{x\text{ref}}$ is always zero. This kind of delay gives the patient time to try to bring his hand to the ball position without robotic support. In the second part of the sequence ($y_{\text{ball}} \leq 0.5$), the force $F_{x\text{ref}}$ is proportional to the distance between the hand and the ball (x_{ball}–x_{hand}) and to the factor (1–y_{ball}), and therefore zero if the patient was able to bring his hand to the ball position during the first sequence. If not, then the supporting force rises when the ball approaches the zero level ($y_{\text{ball}} \rightarrow 0$).

2.10 Passive and active safety

Safety was a main issue during the design of the robot. Passive safety features (no sharp edges, mechanical end stops to guarantee that no joint can exceed the anatomical range of motion, etc.) are combined with active safety features. Four redundant absolute position-sensing potentiometers—one for each joint—allow detecting malfunction of a position sensor. Several surveillance routines are implemented in the software. These include current and speed monitoring, a robot self-collision detection algorithm and several watchdog systems.

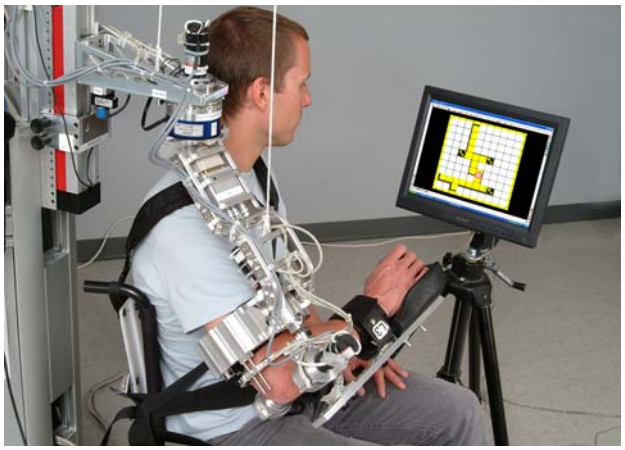

Fig. 8 ARMin prototype that has been used for all experiments described in this paper

Whenever an abnormal event is detected, the safety circuit immediately cuts the power of the motor drives. As the robot is designed with a passive weight compensation system (pulley, rope, and counterweight, see Fig. 8) it does not collapse after power loss. Since all drives are back drivable, the robot can easily be moved manually by a therapist in order to release the patient from a potentially uncomfortable or dangerous posture.

Last but not least, the physiotherapist always observes the training holding a deadman button in his hand. Releasing the button interrupts the motor power and stops the robot immediately. This can also be achieved by pressing one of the three emergency stop buttons. It is expected that future robots will not require a permanent supervision and that the deadman button could be omitted.

Beside patient safety, also safety of the therapist needs to be considered. As the robot does not know the position of the therapist, it is important that the therapist is aware of the danger of collisions with the robot. Nevertheless, the

probability of a severe accident is low because of the fact that the maximal speed of the robot is limited by the surveillance circuit. Furthermore, the therapist can always interrupt the motion by releasing the deadman button. A detailed risk analysis shows that the risk for a patient and a therapist using the robot is acceptable with respect to the expected rehabilitative benefit to the patient.

3 Results

ARMin has been installed at Balgrist University Hospital in Zurich, Switzerland (Fig. 8). After approval of the ethics committee of Zurich, the device first has been tested with healthy subjects. Then, a pilot study including eight hemiplegic and three incomplete spinal cord injured subjects has been carried out, followed by three clinical single-case studies with chronic stroke patients performing intensive robotic training of longer duration. The tests with healthy subjects and the pilot study served to prove the functionality of the device, without looking at possible improvements in the motor performance of the patients. Possible improvements have then been assessed by the clinical studies with the three chronic stroke patients (publication in preparation).

3.1 Control scheme and stability

The dynamic model was used to simulate the overall system and to evaluate the performance of three different controllers: Computed torque, PD in combination with gravity compensation, and PD alone. Sinusoidal reference trajectories ($T = 2\pi$s) where selected as reference trajectories for all four axes. The mean position error was calculated for every axis and for all axes together. Three different conditions where selected. First, the ideal model was used, where ideal means that the plant model (direct dynamic model of robot and human) was equal to the model used for feed forward torque calculation (inverse dynamic model).

Table 4 Mean position errors of different control schemas

	PD + computed torque	PD + gravity compensation	PD
Number of operations per step	8000	150	20
Position error with ideal plant model	0.00007°	0.06°	0.5°
Position error with ideal plant model with sensor discretisation	0.007°	0.06°	0.5°
Position error with falsified plant model with sensor discretisation	0.05°	0.08°	0.5°

Second, the ideal model was used with sensor discretisation. As the encoders deliver a digital signal, no noise was introduced. And third, the direct dynamic model was falsified by increasing the mass of the human arm by 30%, simulating modelling errors. The PD-values where for all cases the same and they have been determined by simulations using the dynamic model (Axis 1: P = 10,000 N/cm, D = 50 Ns/cm; Axis 2: P = 1,000 Nm/rad, D = 10 Nms/rad; Axis 3: P = 1,000 Nm/rad, D = 10 Nms/rad; Axis 4: P = 300 Nm/rad, D = 5 Nms/rad). For all simulations, passive behaviour of the human was assumed. Table 4 summarises the results.

The third condition reflects reality best. In this condition, the computed torque controller does not show significantly better results than the PD controller with gravity compensation, although the computational effort was much higher. In contrast, the pure PD controller required only a few operations, whereas it showed large errors. As a compromise, the PD controller with gravity compensation was chosen and implemented in the robot controller hardware.

In order to find out whether the controller stays stable when the user applies rhythmic disturbances, sinusoidal disturbances acting onto one axis of the robot have been simulated and the position and the velocity error of the simulated robot have been observed. The frequencies of the

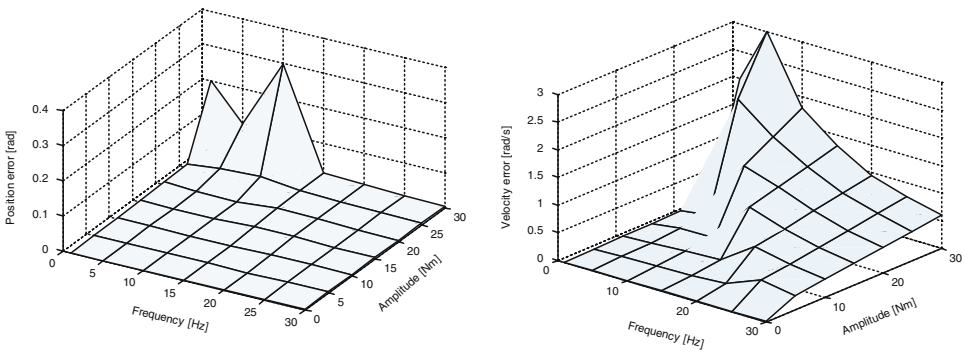

Fig. 9 *Left* Simulated position error with sinusoidal disturbances produced by the human. *Right* Simulated velocity error with sinusoidal disturbances produced by the human. The figure shows when the simulated robot becomes marginally stable, which means that the output is still bounded but vibrations occur

disturbances varied from 0 to 30 Hz with amplitudes varying from 0 to 30 Nm, and the disturbances have been injected at the would point where the user exercises forces onto the robot. For this simulation, the saturation of the motors has been set to 25 Nm.

A series of simulation studies leads to the result that the position error stays small while the velocity error varies with the frequency and amplitude of the disturbance (Fig. 9).

3.2 Functional tests with healthy subjects

Within the tests with healthy subjects, the ROM, the control and the overall functionality have been validated (Table 5). These tests included 20 min' mobilisation therapy and 40 min' game therapy.

3.3 Pilot study with patients

A pilot study was carried out to validate the patient comfort and handling, i.e. whether the robot is adjustable to different patient sizes, whether the cuffs are comfortable for the patients, and whether the patients are able to perform the movement tasks. Furthermore, the patient acceptance and motivation were interrogated.

Using the same protocol as for healthy subjects, the robot has been tested with 11 patients for a cumulative duration of more than 76 h. The robot could easily accommodate subjects with body sizes between 155 and 192 cm. The fixation of a patient in the robot takes approximately 5 min.

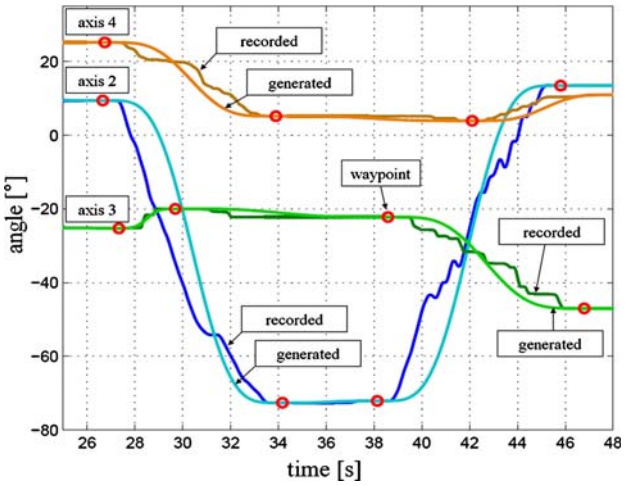

Fig. 10 Recorded trajectories during teach mode and the derived minimized jerk trajectory

Figure 10 shows an example for a trajectory recorded by a therapist and the resulting trajectory after applying the minimum jerk approach. Note that the extreme values of both trajectories correspond with each other.

Figure 11 shows the results of the game therapy with two different hemiplegic patients. A ball has been displayed falling down on the graphical display. The patient had to catch it by moving the virtual hand (Fig. 6, upper right). Subject A was able to catch the ball mostly without any robot support. The robot assisted patient B by pushing the patient with the force F_{xref} towards the ball (Fig. 11), if the patient was not able to catch the ball himself (cf. Chapt. 2.9). Note that the robot support is always delayed relatively to the change in the horizontal ball position. In this

Table 5 Technical data of the device

Payload (Endpoint)	2 kg				
Weight (excl. controller hardware, frame), approx.	6.5 kg				
Repeatability (endpoint)	±3 mm				
Stiffness (endpoint)[a]	>714 N/m				
Minimal apparent mass (endpoint)	240 g				
Bandwidth for small endpoint movements (0.1 m), according to Ellis et al. [3]	2.1 Hz				
Axis data (subject body size 181cm):	Range:	Precision:	Stiffness of the motor/gear unit:	Max torques[b]	Mobilisation torques[c]
Axis 1 (Vertical shoulder rotation)	44° to −59°	0.1°	136 kN/m	57 Nm	10.15 Nm
Axis 2 (Horizontal shoulder rotation)	130° to −50°	0.1°	>1,600 Nm/rad	52 Nm	9.36 Nm
Axis 3 (Internal/external shoulder rotation)	−60° to 95°	0.5°	229 Nm/rad	11 Nm	Not measured
Axis 4 (Elbow flexion/extension)	5° to 119°	0.1°	>1600 Nm/rad	27 Nm	24.36 Nm

[a] Stiffness measured at the endpoint by applying 20 N while the motors are position controlled and a dummy arm was fixed in the device

[b] Torques measured during maximum voluntary contractions of healthy persons

[c] Torque values necessary for mobilisation. Maximum values that occurred during 60 mobilisation movements carried out on three stroke patients

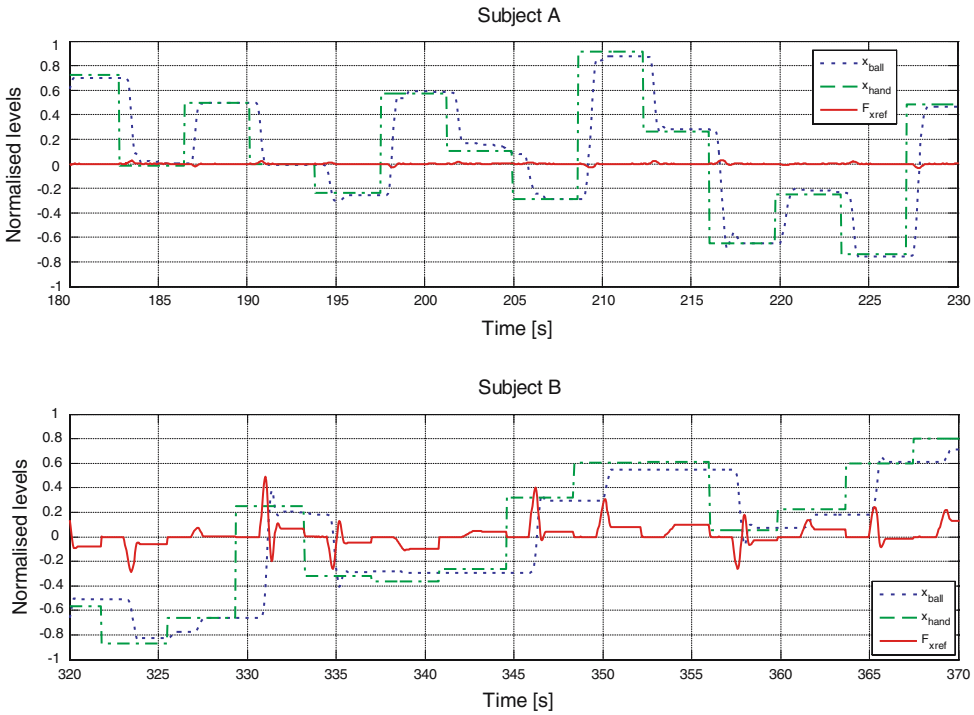

Fig. 11 Movement and force support recorded from two different hemiplecic subjects playing the ball game. Subject A (*upper graph*) does not need support from the robot, while subject B (*lower graph*) needs some support

way, the subject is first encouraged to voluntarily move the virtual hand toward the target. Only when the height of the ball decreases to a level that would not allow the subject to catch the ball, the robot support is activated and guides the arm to the target position.

An important goal was to assess the patient motivation for this kind of therapy. Thus, five patients had to fill out a questionnaire after the therapy sessions. As most of them where not able to read and write, they where interrogated by an independent person. Five questions where asked and the patients could answer with a number between 1 and 6, where 1 means "not at all" and 6 means "very much". This grading system has been selected because it is well known among the patients as it is adapted from the local school system (Table 6).

The pilot study included mobilisation therapy and ball game therapy. The labyrinth game and the ADL training scenarios have been tested with some healthy subjects, but have not been evaluated with patients yet.

Table 6 Questionnaire

Question (translated from German)	Average mark (n = 5)
1. Was the fixation in the robot comfortable?	4.6
2. Did you like to do the mobilisation therapy?	5.25
4. Did you like to play the ball game?	5.0
3. Do you think that this sort of therapy could help you to regain motor function?	5.25
5. What was your overall impression from the device?	5.5

4 Discussion

4.1 Control scheme and stability

It has been shown that the computed torque controller allows a precise position control in the case of an ideal plant. The remaining error is due to the numerical imprecision of the calculations. In the realistic scenario, with discrete sensor information and modelling error, the differences between computed torque and gravity compensation with PD controller become smaller and therefore, the gravity compensation with PD controller is a good compromise between calculation time and precision. The measured position error of 0.1° for axis 1, 2 and 4 and 0.5° for axis 3 is close to the values determined by the simulations and satisfactory for rehabilitation purposes.

Figure 9 shows the position error and the velocity error when the human acts with sinusoidal disturbances at different frequencies. The position error does remain rather small, except when the amplitude gains values above 25 Nm. The reason for this clear increase is that in the simulations the actuator torques were limited to 25 Nm. The velocity error shows more variations. These variations became indeed observable in small, high frequency vibrations that were not visible but produced an audible noise.

Many hours of operation with adjusted PD controller parameters without a patient did not yield instable behaviour. Only high-frequency and high-amplitude external perturbations (e.g. induced by the patient) cannot be compensated by the controller and can cause vibrations (Fig. 9, right).

However, assuming that the bandwidth of human arm movement is limited to 10 Hz [30], such high-frequency and high-amplitude perturbation cannot be induced by the human.

This is not a strict stability proof, but both, the simulation and the experimental results, support the hypothesis that the robot stays stable when it interacts with the human arm.

4.2 Specifications of the device

Most of the specifications for the robot (Table 1) could be fulfilled (Table 5). The ROM of the vertical shoulder rotation is limited by the mechanical construction of the robot.

4.3 Pilot study

The teach-and-repeat mode allows the therapist to easily define an appropriate movement and deliver smooth movements. While the patient is passive during the mobilisation therapy, he or she is active during the ball-game-supported therapy. The results of the questionnaire suggest that the patients like both, the ball game and the mobilisation. The patients rated their fixation in the device with the average mark 4.6, which is significantly lower than the other marks. As the elbow fixation did not cause any problems, this relatively bad mark seems to be related to an uncomfortable shoulder fixation.

In fact, the shoulder actuation module is the most critical component (Fig. 1). It includes 3 actuated DOF and 2 passive DOF, which is advantageous in that the human shoulder is not constrained by the robot fixation. This allows movements of the shoulder in 3 rotary DOF with large ROM. Although the weight of the robot has been compensated by a passive counterbalance system, additional subject-dependent weight and active joint torques produced by the robot will be transferred to the human shoulder as the human arm is closing the open kinematic chain of the robot. During standstill, the distal part of the robot and the human arm beyond the passive axis 5 (Fig. 1) is in a static equilibrium about axis 5. Therefore, the resulting vertical force acting on the shoulder depends on the robot and arm position and the weight of the mechanical components and the human arm. The weight of the distal part of the robot alone induces a vertical shoulder force of approximately 8.5 N (robot arm in a horizontal position, elbow extended). Furthermore, the drives of axes 1–3 produce reaction forces that are transmitted through the shoulder joint to the environment, which further increases the load at the shoulder.

Therefore, patients with instable shoulder joints, e.g. resulting from shoulder subluxations, could not be treated by the robot. Thus, our shoulder actuation approach is acceptable for healthy subjects but problematic for patients with shoulder problems. As many stroke patients suffer from shoulder problems, it has been suggested to modify the shoulder actuation module.

4.4 Prototypes

All simulations and measurements presented in this paper have been performed with the presented 4 DOF version of ARMin (Fig. 8). Derived from the results of this work, a new version with 6 DOF has been set up (Fig. 12). The robot is statically determined and equipped with a new shoulder actuation principle. A system of linkages moves the centre of rotation of the shoulder in the vertical plane, when the arm is lifted. This function is required to provide an anatomically correct shoulder movement and to avoid the shoulder getting mechanically overstressed due to misalignment of the technical and anatomical joint axes when lifting the upper arm above face level. The device is not evaluated yet.

Fig. 12 ARMin II—New version with 6DOF and statically determined shoulder actuation

5 Conclusion and outlook

A new semi-exoskeleton arm rehabilitation robot called ARMin has been developed and tested with numerous stroke and SCI patients. Providing movements in four DOF, ARMin can support spatial arm movements. A patient-cooperative control strategy has been presented and evaluated. It supports the patient only when necessary. In combination with an audiovisual display ARMin can be used to play ball games or to train ADL-related tasks. These methods have the chance to provoke the patients to actively contribute to the movement, increase the motivation of the patient, enhance the intensity of the training and, thus, improve the therapeutic outcome of the therapy compared to conventional training methods. Future technical work will focus on the evaluation of the new shoulder actuation method and the implementation and evaluation of further ADL training tasks. Future clinical work will focus on clinical studies measuring the rehabilitation benefit for the patient. It needs to be demonstrated that the therapeutic outcome of arm therapy with the ARMin robot is higher than the arm therapy delivered by robots with simpler mechanics.

Acknowledgments This study was supported in part by the NCCR for Neuroplasticity and Repair, Project 8, Switzerland. We thank Dr. Gery Colombo from Hocoma AG, Volketswil, Switzerland for his contribution to this work. We also thank the occupational therapists and Prof. Dr. V. Dietz of the Balgrist University Hospital, Zürich, as well as Raphael Suard, Stéphane Kühne, Christina Perndl, Frauke Oldewurtel and Gabriela Kiefer for their contributions to this work.

References

1. Aisen ML, Krebs HI, Hogan N, McDowell F, Volpe BT (1997) The effect of robot-assisted therapy and rehabilitive training on motor recovery following stroke. Arch Neurol 54:443–446
2. Bayona NA, Bitensky J, Salter K, Teasell R (2005) The role of task-specific training in rehabilitation therapies. Top Stroke Rehabil 12:58–65
3. Ellis RE, Ismaeil OM, Lipsett M (1996) Design and evaluation of a high-performance haptic interface. Robotica 14:321–327
4. Emken JL, Bobrow JE, Reinjkensmeyer DJ (2005) Robotic movement training as an optimization problem: designing a controller that can assist only as needed. In: Proceedings of ICORR 2005, 9th international conference rehabilitation robotics, pp 307–312
5. Finley MA, Fasoli SE, Dipietro L, Ohlhoff J, Macclellan L, Meister C et al (2005) Short-duration robotic therapy in stroke patients with severe upper-limb motor impairment. J Rehab Res Dev 42(5):683–691
6. Flash T, Hogan N (1985) The coordination of arm movements: an experimentally confirmed mathematical model. J Neurosci 5(7):1688–1703
7. Harwin W, Loureiro R, Amirabdollahian F, Taylor M, Johnson G, Stokes E, Coote S, Topping M, Collin C et al (2001) In: Marincek C et al (eds) The Gentle/s project: a new method for delivering neuro-rehabilitation, asistive technology-added value to the quality of life AAATE'01.ISO Press, Amsterdam, pp 36–41
8. Herzog W, Nigg BM (1994) Biomechanics of the Muskuloskeletal system. Wiley, Chichester
9. Hesse S, Werner C, Pohl M, Rueckriem S, Mehrholz J, Lingnau ML (2005) Computerized arm training improves the motor control of the severely affected arm after stroke: a single-blinded randomized trial in two centers. Stroke 36(9):1960–1966
10. Hogan N (1985a) Impedance control: an approach to manipulation: Part I—theory. ASME J Dyn Syst Meas Control 107 (11):1–7
11. Hogan N (1985b) Impedance control: an approach to manipulation: Part II—implementation. ASME J Dyn Syst Meas Control 107(11):8–16
12. Hogan N (1985c) Impedance control: an approach to manipulation: Part III—applications. ASME J Dyn Syst Meas Control 107(11):17–24
13. Hogan N, Krebs HI, Rohrer B, Palazzolo JJ, Dipietro L, Fasoli SE, Stein J, Hughes R, Frontera WR, Lynch D, Volpe BT (2006) Motions or muscles? Some behavioral factors underlying robotic assistance of motor recovery. J Rehab Res Dev 43(5):605–618
14. Jack D, Boian R, Merians AS, Tremaine M, Burdea GC, Adamovich SV, Recce M, Poizner H (2001) Virtual reality-enhanced stroke rehabilitation. IEEE Trans Neural Syst Rehab Eng 9(3):308–318
15. Jung-Hoon H, Ronald CA, Dong-Soo K (2003) Mobile robots at your fingertip: Bezier curve on-line trajectory generation for supervisory control. IEEE International conference of intelligent robots and systems
16. Krebs HI, Hogan N, Aisen ML, Volpe BT (1998) Robot-Aided Neurorehabilitation. IEEE Trans Rehab Eng 6:75–87
17. Kwakkel G, Wagenaar RC, Koelman TW, Lankhorst GJ, Koetsier JC (1997) Effects of intensity of rehabilitation after stroke. A research synthesis. Stroke 28:1550–1556
18. Kwakkel G, Wagenaar RC, Twisk JWE, Langkhorst GJ, Koetsier JC (1999) Intersity of leg and arm training after primary middlecelebral artery stroke: a randomised trial. Lancet 35:191–196
19. Kwakkel G, Kollen BJ, Wagenaar RC (2002) Long therm effects of upper and lower limb training after stroke: a randomised trial. J Neurol Neurosurg Psychiat 72:473–479
20. Luft AR, McCombe-Waller S, Whitall J, Forrester LW, Macko R, Sorkin JD, Schulz JB, Goldberg AP, Hanley DF (2004) Repetitive bilateral arm training and motor cortex activation in chronic stroke—a randomized controlled trial. JAMA 292:1853–1861
21. Lum PS, Burgar CG, Shor PC, Majmundar M, Van der Loos M (2002) Robot-assisted movement training compared with conventional therapy techniques for the rehabilitation of upper-limb motor function after stroke. Arch Phys Med Rehab 83(7):952–959
22. Langhammer B, Stanghelle JK (2000) Bobath or motor relearning programme? A comparison of two different approaches of physiotherapy in stroke rehabilitation: a randomised controlled study. Clin Rehabil 14:361–369
23. Mihelj M, Nef T, Riener R (2007) A novel paradigm for patient cooperative control of upper limb rehabilitation robots. Adv Robot 21(8):843–867
24. Nef T, Colombo G, Riener R (2005) ARMin—robot for movement therapy of the upper extremities. Automatisierungstechnik 53(12):597–606
25. Platz T (2003) Evidenzbasierte Armrehabilitation: Eine systematische Literaturübersicht. Nervenarzt 74:841–849
26. Prange GB, Jannink MJ, Groothuis-Oudshoorn CG, Hermens HJ, IJzerman MJ (2006) Systematic review of the effect of robot-aided therapy on recovery of the hemiparetic arm after stroke. J Rehabil Res Dev 43(2):171–184

27. Riener R, Nef T, Colombo G (2005) Robot-aided neurorehabilitation for the upper extremities. Med Biol Eng Comput 43:2–10
28. Riener R, Lünenburger L, Jezernik S, Anderschitz M, Colombo G, Dietz V (2005) Cooperative subject-centered strategies for robot-aided treadmill training: first experimental results. IEEE Trans Neural Syst Rehab Eng 13:380–393
29. Sanchez RJ, Liu J, Rao S, Shah P, Smith R, Rahman T, Cramer SC, Bobrow JE, Reinkensmeyer DJ (2006) Automating arm movement training following severe stroke: functinal exercise with quantitative feedback in a gravity-reduced environment. IEEE Trans Neural Syst Rehabil Eng 14(3):378–389
30. Schouten AC, de Vlugt E, van der Helm FCT, Brouwn GG (2004) Optimal posture control of a musculo-skeletal arm model. Biol Cybern 84(2):143–152
31. Siciliano B, Villani L (1999) Robot force control. Kluwer, Boston
32. Stein J, Krebs HI, Frontera WR, Fasoli SE, Hughes R, Hogan N (2004) Comparison of two techniques of robot-aided upper limb exercise training after stroke. Am J Phys Med Rehabil 83(9):720–728
33. Sunderland A, Tinson DJ, Bradley EL, Fletcher D, Langton HR, Wade DT (1992) Enhanced physical therapy improves recovery of arm function after stroke. A randomised clinical trial. J Neurol Neursurg Psychiatry 55:530–535
34. Winstein CJ, Rose DK, Tan SM, Lewthwaite R, Chui HC, Azen SP (2004) A randomized controlled comparison of upper-extremity rehabilitation strategies in acute stroke: a pilot study of immediate and long-term outcomes. Arch Phys Med Rehab 85(4):620–628
35. Winter D (1989) Biomechanics and motor control of human movement, 2 edn. Wiley, New York